Energy & Environmental Science

Accepted Manuscript

ROYAL SOCIETY OF CHEMISTRY

www.rsc.org/ees

Journal Name

ARTICLE

How simple are the models of Na-intercalation in aqueous media?

Jeongsik Yun,[a] Jonas Pfisterer,[a] Aliaksandr S. Bandarenka*[,a,b]

Received 00th January 20xx,
Accepted 00th January 20xx

DOI: 10.1039/x0xx00000x

www.rsc.org/

Intercalation is among interesting phenomena changing the everyday life with a remarkable speed. Numerous generations of modern batteries use it and markedly contribute to the portfolio of energy materials for future sustainable energy provision. Na-ion batteries operating in aqueous media, being presumably the "number two" compared to other alternatives for portable and automotive applications, are probably among potential leaders in the case of future larger-scale energy storage schemes, specifically because of safety and sustainability issues. However, there is a certain lack of detailed understanding of such systems. In this work, using model electrodes we further emphasise that not only the electrode materials themselves determine the performance of intercalation electrodes. Surprisingly, comparatively slight changes in the electrolyte composition and solvation effects can very radically control intercalation of alkali metal cations. Therefore, it would be stimulating to adjust existing strategies in designing future aqueous battery systems. Several examples are given using one of the state of the art cathode materials, $Na_2Ni[Fe(CN)_6]$, with model electrodes prepared as quasi-uniform thin films.

Introduction

Solar and wind energy systems significantly contribute to the energy provision schemes already nowadays.[1-4] However, more effective solutions of the so-called "generation versus consumption" problem are required to facilitate their further development. Rechargeable batteries are a part of the answer to this challenge as they are, in general, very convenient means for energy storage thanks to their relative affordability, flexibility, high energy conversion efficiency and simple maintenance.[5,6]

Intercalation materials for lithium ion batteries remain probably among the most attractive ones for portable devices and automotive applications.[7-9] Nevertheless, for larger-scale stationary energy storage systems, several key issues should be additionally considered. For instance, one of them is related to the sustainability factors.[10] It has been roughly estimated that in order to address the so-called "TW-challenge" using just Li-ion batteries, ~160 years of current lithium production would be necessary.[11] While there is a certain capability to increase the rate of production of this metal substantially, it is nowadays clear that its fast accumulation for various stationary applications might be problematic. The second issue is associated to the current use of flammable organic electrolytes in Li-ion batteries. Safety problems upon scaling-up are often of non-trivial complexity, increasing the maintenance costs and the total system price in this case.[12-16]

A viable alternative for stationary large-scale storage applications is to use Na-ion batteries, where electrode materials operate in aqueous media.[17-24] This type of devices has attracted great attention with a constantly increasing amount of publications, as thoroughly reviewed recently by Kim et al.[25] Accumulation of Na in amounts necessary to address the TW-challenge seems to be more than one order of magnitude faster if compared with lithium.[11] Additionally, aqueous electrolytes would gradually minimise safety risks. However, further development and optimisation of functional electrode materials in this area requires detailed understanding of processes which control Na-intercalation and de-intercalation, including the interfacial charge transfer. For this, model systems and electrodes as well as their comprehensive *in-situ* characterisation are necessary.

In this work, using model electrodes consisting of electrochemically deposited thin films of one of the state-of-the-art cathode materials, namely $Na_2Ni[Fe(CN)_6]$ (a typical representative of so-called Prussian blue analogues),[26,27] we demonstrate that intercalation of Na and its reversibility in the cathodic and anodic cycles are largely influenced by the nature of anions present in the electrolytes. On the other hand, the electrode potential required for intercalation is determined not only by the electrode material itself; it is directly proportional to the hydration (solvation) energy of cations. Implications to the development of new Na-ion battery systems are briefly discussed.

[a] Physik-Department ECS, Technische Universität München, James-Franck-Straße 1, 85748 Garching, Germany
[b] Nanosystems Initiative Munich (NIM), Schellingstraße 4, 80799 Munich, Germany
* Corresponding Author: tel. +49 (0) 89289 12531, email bandarenka@ph.tum.de
Electronic Supplementary Information (ESI) available: experimental details, additional experimental data and data analysis. See DOI: 10.1039/x0xx00000x

Experimental

$Na_2Ni[Fe(CN)_6]$ thin films were deposited onto AT-cut Au quartz crystal wafers (Stanford Research Systems) from the solution of 0.25 M Na_2SO_4 containing 0.5 mM $K_3Ni[Fe(CN)_6]$ and 0.5 mM $NiCl_2{\cdot}6H_2O$ by cycling the potential in the range from 0.05 V to 0.85 V at the scan rate of 50 mV/s for ~60 cycles as shown in Figures 1A,B. All chemicals and solvents utilized in this work were used without further treatments and listed with full details in the electronic supplementary information. The experiments were performed in a typical glass cell exploiting a three electrode setup using a Bio-Logic VSP-300 potentiostat and a QCM 200 (Stanford Research Systems) electrochemical quartz crystal microbalance (EQCM). Electrode potentials were referred to a Ag/AgCl (SSC) reference electrode. A Pt wire was used as a counter electrode.

Cyclic voltammetry (CV), EQCM measurements and common battery tests were performed using different electrolytes including 1 M Na_2SO_4, 0.25 M Na_2SO_4, 0.25 M NaCl, 0.25 M $NaNO_3$, 0.25 M $NaClO_4$ and 0.25 M NaOAc (sodium acetate). Moreover, in order to determine the onset potential for intercalation of various alkali metal cations, further experiments also involved different 0.25 M aqueous solutions of MNO_3 where (M = Li, Na, K, Rb, or Cs) at the scan rate of 50 mV/s. Electrochemical Impedance Spectroscopy (EIS) characterisation of the $Na_2Ni[Fe(CN)_6]$ thin films in 0.25 M Na_2SO_4 electrolytes were conducted using AC probing frequencies between 10 kHz and 0.5 Hz with a 10 mV amplitude of the probing signals in the potential range between 0.1 V and 0.8 V. The output of the fitting procedure was controlled by the root-mean-square deviations and estimated individual parameter errors using home-made "EIS Data Analysis 1.0" software to ensure the validity of the model and correctness of the fitting, as described in detail elsewhere.[28,29]

The morphology and uniformity of the deposited thin films

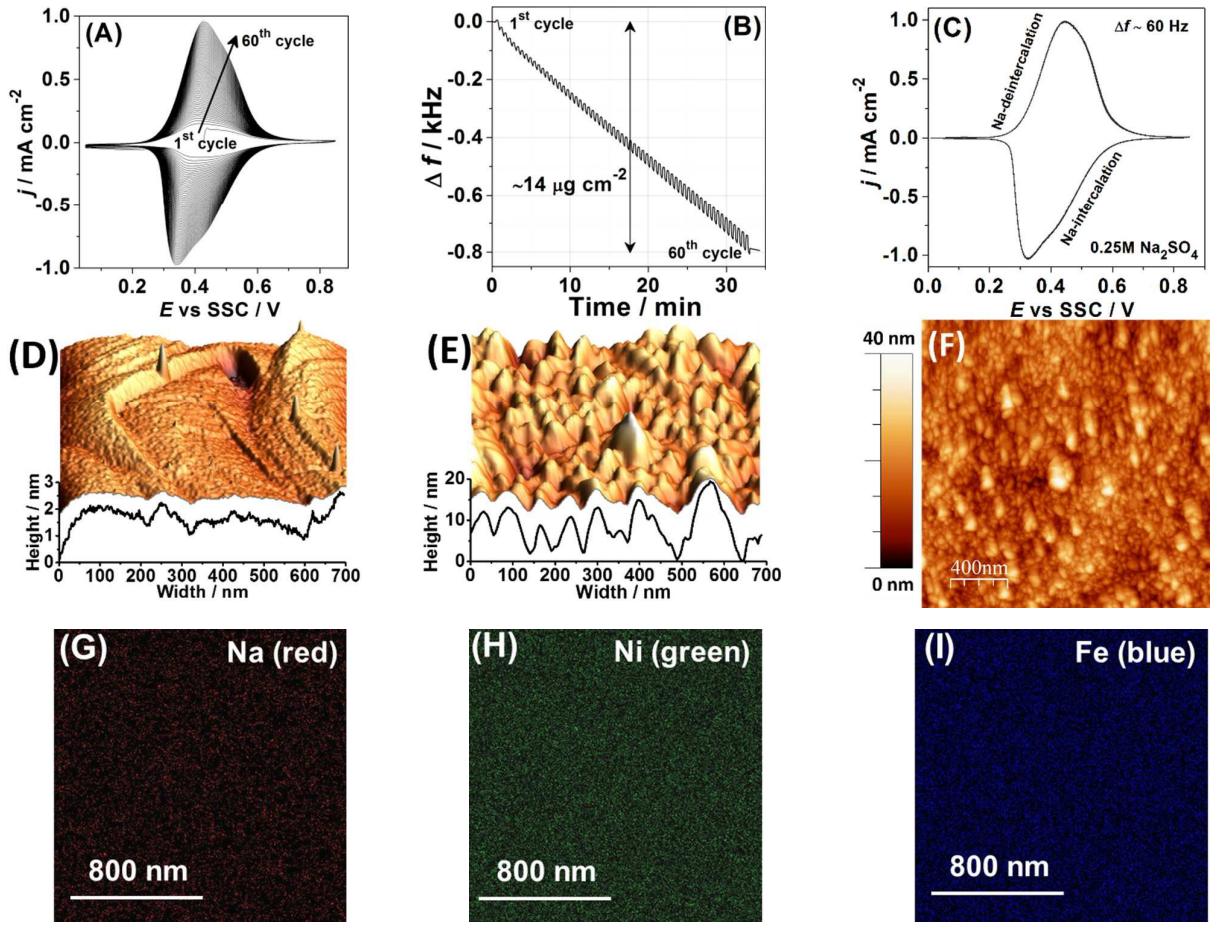

Figure 1. Characterisation of the $Na_2Ni[Fe(CN)_6]$ thin films. (A) A typical cyclic voltammogram obtained during film deposition and (B) the corresponding electrode mass change, d*E*/dt = 50 mV/s. (C) A typical cyclic voltammogram characterising Na-intercalation/de-intercalation in aqueous 0.25 M Na_2SO_4 electrolyte. (D-F) AFM pictures comparing a reference metal single crystal surface (D) before and (E,F) after deposition of the $Na_2Ni[Fe(CN)_6]$ thin films. (G-I) Distribution of (G) Na, (H) Ni and (I) Fe in the resulting film (see electronic supplementary information for further details).

were investigated by SEM, Electron Microprobe and AFM. The Atomic Force Microscope, utilized in this work, was a multimode EC-STM/AFM instrument (Veeco VI) with a Nanoscope IIID controller using the Nanoscope 5.31r1 software. All measurements were conducted in tapping mode (AFM-tips BRUKER RTESP-300). SEM and Electron Microprobe images were obtained with a 20 kV beam using "Mira" from Tescan, Czech Republic with electron microprobe "INCA Energy 350" from Oxford Instruments Analytical, UK.

Further detailed information on experimental procedures, instrumentation and chemicals, are available within the electronic supplementary information.

Results and discussion

The following electrochemical reaction was used to form thin films of $Na_2Ni[Fe(CN)_6]$ under potentiodynamic conditions, as additionally described in detail in the electronic supplementary information:

$2Na^{+}_{(aq.)} + Ni^{2+}_{(aq.)} + [Fe^{III}(CN)_6]^{3-}_{(aq.)} + 1e^{-} \rightarrow Na_2Ni[Fe^{II}(CN)_6]_{(solid)}$

Figure 1A shows a typical cyclic voltammogram (CV), which characterises the deposition process. It should be noted here that CVs in each subsequent Figure, related to the same type of experiments (for instance CVs of Na-intercalation in 0.25 M Na_2SO_4 solutions), are shown for different sets of experiments intentionally in order to demonstrate a good reproducibility; however, some possible stability issues are not taken into account, as they are outside of the scope of this work. Anodic and cathodic peaks in the CV shown in Figure 1A are due to the changes in the oxidation state of Fe in the forming $Na_2Ni[Fe(CN)_6]$ film. It can be seen from Figure 1A that the peak current increases with the potential cycles. The associated net electrode mass change measured using a quartz crystal microbalance is shown in Figure 1B. The comparison of the resulting mass change at the end of the deposition process (~14 μg cm^{-2}) and the integrated charge from the CV (~4.6 mC cm^{-2}) gives within ~5% of accuracy the expected molar weight for $Na_2Ni[Fe(CN)_6]$ (note that oscillations seen in Figure 1B are due to intercalation and de-intercalation of sodium during the film formation). Figure 1C shows a typical CV of the $Na_2Ni[Fe(CN)_6]$ film in a pure aqueous 0.25 M Na_2SO_4 electrolyte characterising Na-intercalation/de-intercalation (corresponding net electrode mass change is ~1 μg cm^{-2}, which is close to the expected one, considering that only 50% of sodium is exchanged in the complete cycle). The resulting electrodes are relatively smooth (see the morphology and topology in Figures 1D-F and the electronic supplementary information), with uniform distribution of the key elements, Na, Ni and Fe, as revealed by the electron microprobe technique (Figures 1G-I).

A generally accepted scheme of Na-intercalation and de-intercalation in aqueous systems in the case of $Na_2Ni[Fe(CN)_6]$

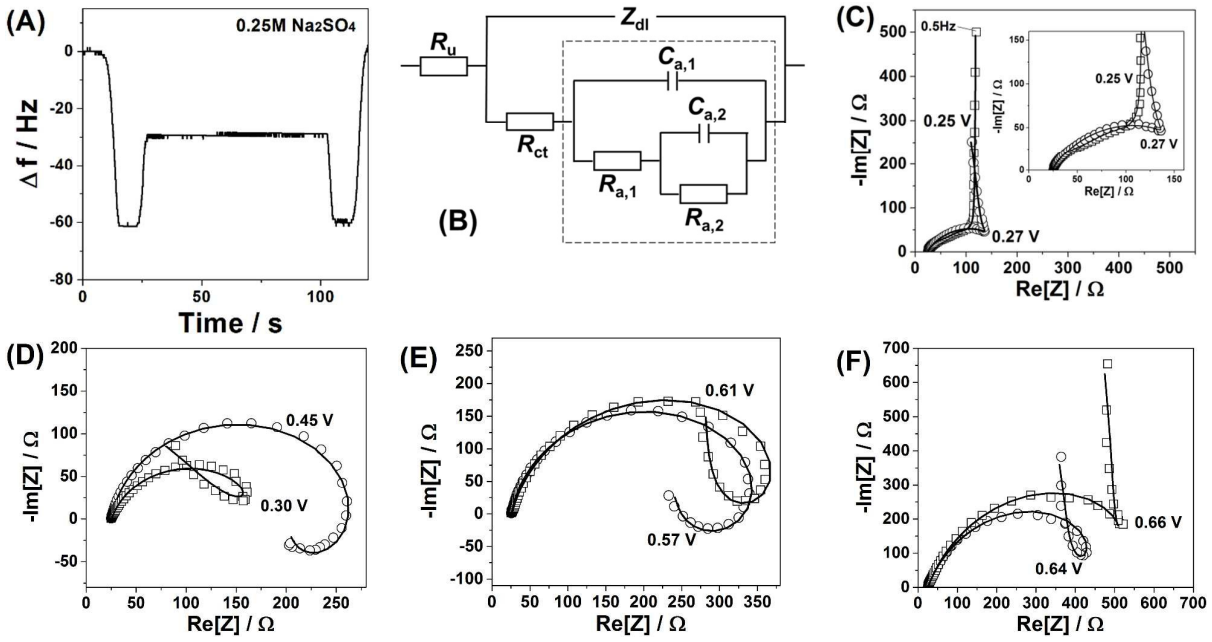

Figure 2. Characterisation of the $Na_2Ni[Fe(CN)_6]$ thin films using impedance spectroscopy. (A) A typical electrode mass change curve confirming quasi-stationarity of the system within the time necessary to record one impedance spectrum. (B) Equivalent electric circuit reflecting the 3-stage mechanism (R_u - uncompensated resistance, Z_{dl} - impedance of the double layer, R_{ct} - charge transfer resistance, other R and C elements are adsorption (pseudo)resistances and (pseudo)capacitances, respectively, which are given by complex combinations of physico-chemical parameters of adsorption/desorption (see text for details). (C-F) Examples of impedance spectra (open symbols) at different electrode potentials together with the fitting (solid lines) to the model shown in (B).

cathode material is given as follows:[25]

$$NaNi[Fe^{III}(CN)_6] + Na^+ + e^- \leftrightarrow Na_2Ni[Fe^{II}(CN)_6] \quad \text{Eq. 1}$$

This scheme describes Na-intercalation as a very simple one-stage process, in which neither solvent nor other electrolyte components play an essential role. In order to explore the validity of the mechanism presented above in more detail, we have performed an electrochemical impedance spectroscopy study enforced with nano-gravimetry. The latter was used to particularly ensure the required quasi-stationarity of the system during the measurements. Figure 2A shows a typical electrode mass change during the voltammetric cycling and subsequent potentiostatic modes (the latter is referred to the rather convenient for the further comparison situation when only ~50% of the intercalated sodium is exchanged, i.e. a "half-charged"/"half-discharged" state). As can be seen from the Figure 2A, after the electrode potential had been fixed, the electrode mass remained practically unchanged during the time required to obtain an impedance spectrum (~1 min). Additionally, the Krammers-Kronig tests did not reveal significant problems with spectra quality.

Surprisingly, impedance spectra recorded at different electrode potentials at which Faradaic processes take place do not support the hypothesis about the simple one-stage mechanism of the interfacial process. Typical "loops" which can be seen in the spectra (Figures 2C-F) suggest *at least* a 3-stage mechanism involving two reversible "intermediate steps" with the interfacial charge transfer, followed by a step which does not contribute to the net charge transfer through the interface (see electronic supplementary information for further details). The unique relation of the spectra shapes and the multi-stage mechanisms is well-known and protocolled for various systems, as summarised in ref [30]. Furthermore, a relatively simple physical model which reflects the above-mentioned 3-stage mechanism (Figure 2B) fits well all the spectra for all the measured potentials, additionally verifying that the observed spectra shapes are not an experimental artifact due to e.g. contaminations, non-stationarity or non-linearity effects. Thus, a more complex model should be taken into account.

As the first approximation we propose the following three-stage mechanism capable to explain the impedance data (for the simplicity only de-intercalation is formally discussed, while all three steps are quasi-reversible):

(1) Electroactive step, i.e. oxidation of Fe^{II}, which proceeds comparatively fast due to a good electronic conductivity of the film (we use some arbitrary schematic designations in the equations below):

$$Na_2Ni[Fe^{II}(CN)_6] - e^- \leftrightarrow Na_2Ni[Fe^{III}(CN)_6]^+ \quad \text{Eq. 2}$$

(2) Specific adsorption step, which can be considered as temporary compensation of the excessive positive electrode charge due to relatively slow Na^+ de-intercalation (this step is probable to distinguish as separate one in EIS, as the mass transport in solids is relatively slow compared to one in liquids, and the change in the oxidation state of Fe in the film is in turn faster than the mentioned compensation from the electrolyte side):

$$2Na_2Ni[Fe^{III}(CN)_6]^+ + SO_4^{2-} \leftrightarrow (Na_2Ni[Fe^{III}(CN)_6])_2SO_4 \quad \text{Eq. 3}$$

(3) "Non-electroactive step" (no net interfacial charge transfer), Na^+ and SO_4^{2-} ions leave the surface:

$$(Na_2Ni[Fe^{III}(CN)_6])_2SO_4 \leftrightarrow 2\ Na^+ + SO_4^{2-} + 2NaNi[Fe^{III}(CN)_6] \quad \text{Eq. 4}$$

Importantly, the suggested mechanism involves the electrolyte components, namely anions. If sodium intercalation and de-intercalation indeed depend on the electrolyte composition, some key kinetic properties should be affected by changing the nature of the anions or their concentrations accordingly. Indeed, Figure 3A further supports this hypothesis.

Figure 3A shows how the nature of anions influences the peak shapes and so-called voltammetric reversibility, i.e. it reveals how fast intercalation and de-intercalation of sodium are as a function of the electrolyte composition. Noticeably, the corresponding peak separation becomes more and more evident if more "asymmetric" anions and/or anions with a lower net negative charge density are used, i.e. SO_4^{2-} < Cl^- < NO_3^- < ClO_4^- < OAc^-. This trend cannot be easily explained by some electrolyte conductivity issues, as e.g. aqueous solutions

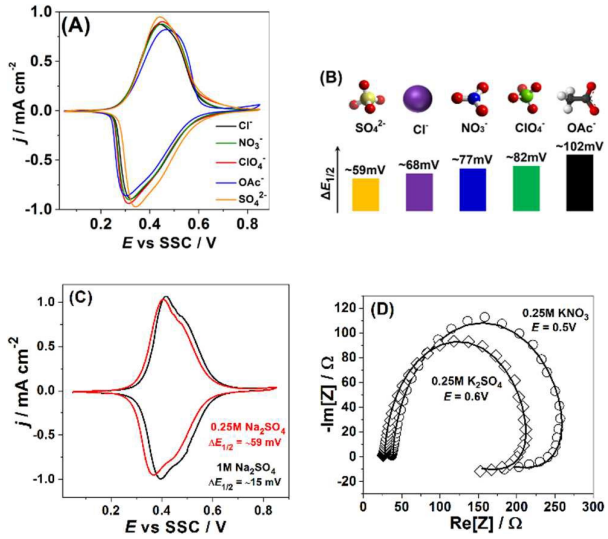

Figure 3. Influence of the nature of anions and their concentration on reversibility and mechanism of sodium intercalation to $Na_2Ni[Fe(CN)_6]$. (A) Typical CVs in presence of different anions, dE/dt = 50 mV/s. (B) Qualitative correlations between the $\Delta E_{1/2}$, and the net charge density as well as the "symmetry" of the anions. (C) Effect of the sulfate-anion concentration on the voltammetric reversibility. (D) Impedance spectra (open symbols) and corresponding fitting results (solid lines, model is shown in Figure 2B) in presence of KNO_3 and K_2SO_4.

of Na_2SO_4, NaCl and $NaNO_3$ of these concentrations have very similar (within 2-3%) conductivities. However, the above-elucidated trend is in qualitative accordance with Equation 3, where efficient compensation of the excessive "electrode charge" is necessary for the fast sodium exchange at the interface. Figure 3B additionally illustrates this effect. In that picture the differences between the potentials of the "half-charged" and "half-discharged" states, $\Delta E_{1/2}$, are given for each anion used in this study.

Further evidences supporting the importance of the electrolyte composition for sodium interfacial transfer are given in Figure 3C. The increase in the concentration of Na_2SO_4 not only shifts the potentials of Na intercalation / de-intercalation, as expected from the common rules; it also decreases the degree of CV-irreversibility between the "charging" and "discharging" cycles. Again, this effect cannot be easily explained by e.g. some electrolyte conductivity issues. It is even not proportional to the increase in the electrolyte conductivity (~2 times). However, it is well in accordance with the requirement of fast and effective compensation of the effective charge at the interface (Eq. 3) and questioning the simple mechanism represented by Equation 1.

Moreover, Figure 3D demonstrates that the observed shapes of the impedance spectra are not because of some specific electrolyte composition: changing the anions or cations does seem to be critical for the mechanism of the interfacial charge transfer itself in this case, further reducing the probability of misinterpretation of the CVs shown in Figures 3A,C. Therefore, even relatively small changes in the electrolyte composition can play a very essential role in the interfacial charge transfer. Figure 4A schematically illustrates the importance of the intermediate interfacial charge compensation from the electrolyte side during intercalation/de-intercalation. Additionally, Figure 4B shows that the performance of an optimised system, even at a high C-rate (180 C), is very good, with the specific capacity (~80 $mAhg^{-1}$) being only ~5% lower than the theoretically possible value for this material (see more experimental data in Figures S8-S10 of the electronic supplementary information).

Another important parameter controlling the performance of the secondary intercalation batteries is the potential at which intercalation starts. Very straightforward expectations about the capability of alkali metal cations to insert into the $Na_2Ni[Fe(CN)_6]$-like structures from the electrolyte side are associated with the size of the intercalating cations[31-33]. According to these expectations, the larger the cation the more difficult it is to be intercalated into the solid state structure; though it is still possible for all the cations from Li^+ to Cs^+ to do so in the case of $Na_2Ni[Fe(CN)_6]$ (see schematics in Figure 5A). Corresponding to this model, Cs^+ should intercalate at much more negative potentials compared to e.g. Li^+. However, what is observed experimentally is exactly the opposite, as was partially reported previously.[34,35]

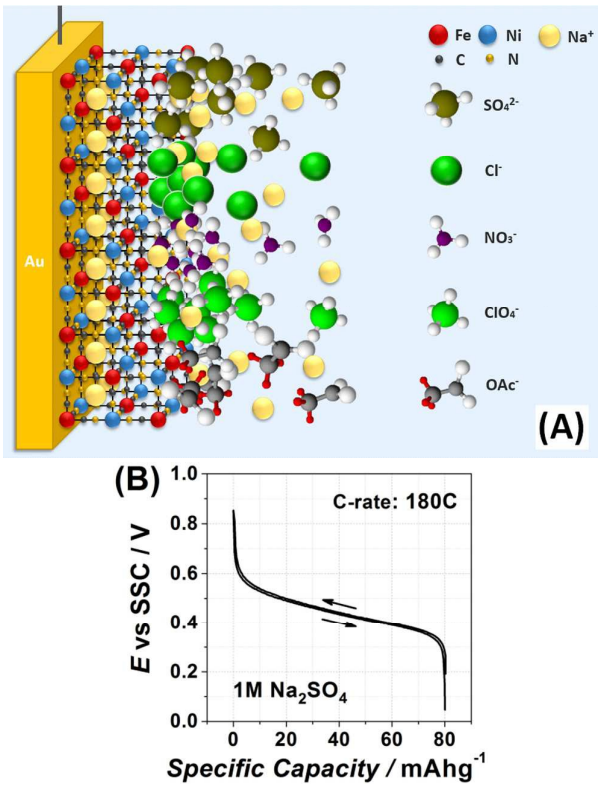

Figure 4. (A) Schematic representation of the situation when the temporal and spatial charge compensation is critical to enhance the interfacial charge transfer (see text for details). Due to a slower diffusion of alkali metal cations in the solid with respect to the liquid electrolyte side (illustrated in the Figure as a deficiency of Na-ions in the solid thin film) the comparatively immediate change in the oxidation state of Fe-atoms in the film requires a fast response from the electrolyte side. The latter would depend on the concentration, effective charge density and the geometry of e.g. anions. (B) Galvanostatic charge and discharge curves at 180 C for $Na_2Ni[Fe(CN)_6]$ electrodes in 1 M Na_2SO_4. The galvanostatic cycling even at this very high C-rate shows a very low hysteresis resulting in high energy efficiencies.

Figure 5B displays typical cyclic voltammograms for $Na_2Ni[Fe(CN)_6]$ in 0.25 M aqueous solutions of MNO_3 where (M = Li, Na, K, Rb, or Cs). It can be seen from the Figure that intercalation is possible for all five alkali metal cations. Moreover, our quartz crystal microbalance data (not shown here) suggest that even after tens of initial cycles the net reaction can be fairly described as follows:

$$NaNi[Fe^{III}(CN)_6] + M^+ + e^- \leftrightarrow MNaNi[Fe^{II}(CN)_6]$$

(where M = Li, K, Rb, Cs) i.e. only approximately half of the sodium is replaced by the other alkali metal cations.

Surprisingly, despite the biggest cation radius of Cs^+, its insertion starts at the most positive electrode potentials followed by Rb^+, K^+, Na^+, and Li^+. Evidently, not only the cation size but other physico-chemical parameters control the potential of their insertion. One of these parameters might be the ion hydration energy. Indeed if the potential of the half charged state is plotted as a function of the alkali metal cation

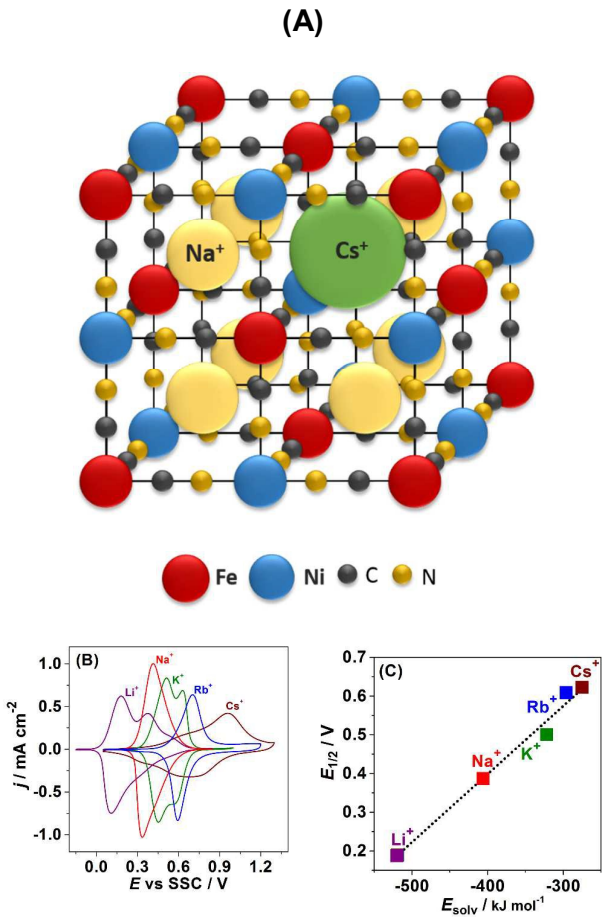

Figure 5. Cation size versus cation solvation effect on intercalation of alkali metal cations into $Na_2Ni[Fe(CN)_6]$. (A) Schematics of the $Na_2Ni[Fe(CN)_6]$ crystal structure demonstrating that even Cs^+ can be inserted (all atoms have approximately realistic relative sizes). (B) Typical cyclic voltammograms for $Na_2Ni[Fe(CN)_6]$ in 0.25 M aqueous solutions of MNO_3 where (M = Li, Na, K, Rb, or Cs), dE/dt = 50 mV/s. (C) The potential of the "half-charged" state as a function of the alkali metal cation hydration energy.

hydration energy, a statistically relevant linear correlation is observed (Figure 5C).

Conclusions

In summary, we have further emphasised the importance of the electrolyte composition for the kinetics and mechanisms of the interfacial charge transfer during intercalation / de-intercalation of sodium in the cathode materials for the Na-ion batteries. Answering the question stated in the title of this manuscript, the commonly accepted models of Na-intercalation in aqueous media, including a variety of theoretical ones, are likely too much oversimplified affecting the strategies of the developing of new materials for large-scale energy storage schemes. In particular, the nature of the anions present in the electrolyte significantly influences the intercalation / de-intercalation. On the other hand, solvation effects are probably among the main parameters governing the potential of the alkali metal intercalation.

Consequently, more sophisticated models for Na-intercalation in aqueous media need to be further elaborated to ascribe the observed trends. This will enhance our fundamental understanding and thus the performance of such Na-ion battery systems in the future.

Acknowledgements

Financial support from SFB 749, the cluster of excellence Nanosystems Initiative Munich (NIM) is gratefully acknowledged.

References

1 V. S. Arunachalam and E. L. Fleischer, *MRS Bull.*, 2008, **33**, 264-276.
2 J. P. Holdren, *Science*, 2007, **315**, 737-737.
3 D. Ginley, M. A. Green and R. Collins, *MRS Bull.*, 2008, **33**, 355-364.
4 Z. G. Yang, J. L. Zhang, M. C. W. Kintner-Meyer, X. C. Lu, D. W. Choi, J. P. Lemmon and J. Liu, *Chem. Rev.*, 2011, **111**, 3577-3613.
5 B. Dunn, H. Kamath and J. M. Tarascon, *Science*, 2011, **334**, 928-935.
6 G. L. Soloveichik, *Annu. Rev. Chem. Biomol.*, 2011, **2**, 503-527.
7 M. Armand and J. M. Tarascon, *Nature*, 2008, **451**, 652-657.
8 J. M. Tarascon and M. Armand, *Nature*, 2001, **414**, 359-367.
9 V. Etacheri, R. Marom, R. Elazari, G. Salitra and D. Aurbach, *Energy Environ. Sci.*, 2011, **4**, 3243-3262.
10 J. Y. Luo and Y. Y. Xia, *Adv. Funct. Mater.*, 2007, **17**, 3877-3884.
11 P. C. K. Vesborg, T. F. Jaramillo, *RSC Adv.*, 2012, **2**, 7933-7947.
12 Y. Wu, X. Dai, J. Ma, Y. Chen, Lithium Ion Batteries: Practice and Applications; *Chemical Industry Press: Beijing*, 2004.
13 W. Tang, Y. S. Zhu, Y. Y. Hou, L. L. Liu, Y. P. Wu, K. P. Loh, H. P. Zhang and K. Zhu, *Energy Environ. Sci.*, 2013, **6**, 2093-2104.
14 Z. Chang, Y. Q. Yang, M. X. Li, X. W. Wang and Y. P. Wu, *J. Mater. Chem. A*, 2014, **2**, 10739-10755.
15 W. Tang, L. L. Liu, Y. S. Zhu, H. Sun, Y. P. Wu and K. Zhu, *Energy Environ. Sci.*, 2012, **5**, 6909-6913.
16 Y. G. Wang, J. Yi and Y. Y. Xia, *Adv. Energy Mater.*, 2012, **2**, 830-840.
17 H. L. Pan, Y. S. Hu and L. Q. Chen, *Energy Environ. Sci.*, 2013, **6**, 2338-2360.
18 S. Ferlay, T. Mallah, R. Ouahes, P. Veillet and M. Verdaguer, *Nature*, 1995, **378**, 701-703.
19 Y. H. Lu, L. Wang, J. G. Cheng and J. B. Goodenough, Chem. Commun., 2012, **48**, 6544-6546.
20 L. Wang, Y. H. Lu, J. Liu, M. W. Xu, J. G. Cheng, D. W. Zhang and J. B. Goodenough, *Angew. Chem. Int. Edit*, 2013, **52**, 1964-1967.
21 H. W. Lee, R. Y. Wang, M. Pasta, S. W. Lee, N. Liu and Y. Cui, *Nat. Commun.*, 2014, **5**.
22 C. D. Wessells, R. A. Huggins and Y. Cui, *Nat. Commun.*, 2011, **2**.
23 M. Pasta, C. D. Wessells, R. A. Huggins and Y. Cui, *Nat. Commun.*, 2012, **3**.
24 M. Pasta, C. D. Wessells, N. Liu, J. Nelson, M. T. McDowell, R. A. Huggins, M. F. Toney and Y. Cui, *Nat. Commun.*, 2014, **5**.
25 H. Kim, J. Hong, K.-Y. Park, H. Kim, S.-W. Kim, K. Kang, *Chem. Rev.*, 2014, **114**, 11788−11827.

26 C. D. Wessells, S. V. Peddada, R. A. Huggins and Y. Cui, *Nano Lett.*, 2011, **11**, 5421-5425.
27 X. Y. Wu, Y. L. Cao, X. P. Ai, J. F. Qian and H. X. Yang, *Electrochem. Commun.*, 2013, **31**, 145-148.
28 A. S. Bondarenko, *Anal. Chim. Acta*, 2012, **743**, 41.
29 A. S. Bondarenko and G. A. Ragoisha, *in Progress in Chemometrics Research*, ed. A. L. Pomerantsev, 2005, 89–102.
30 A. Lasia, *Electrochemical Impedance Spectroscopy and its Applications*, Springer-Verlag New York, 2014, 367.
31 K. Itaya, I. Uchida, and V. D. Neff, "Electrochemistry of polynuclear transition metal cyanides: prussian blue and its analogues", Accounts of Chemical Research®, 1986, **19**, no. 6, 162–168.
32 N. Bagkar, C. A. Betty, P. A. Hassan, K. Kahali, J. R. Bellare, J. V. Yakhmi, *Thin Solid Films*, 2006, **497**, no. 1-2, 259–266.
33 W. Jin, A. Toutianoush, M. Pyrasch et al., *J. Phys. Chem. B*, 2003, **107**, no.44, 12062–12070, 2003.
34 M. A. Malik, P. J. Kuelsza and R. Marrassi. *Electrochimica Acta*, 2004, **49**, 4253–4258.
35 Wei Chen, Jian Tang, and Xing-Hua Xia, *J. Phys. Chem. C*, 2009, **113**, 21577–21581.

One sentence of text, maximum 20 words, highlighting the novelty of the work

This work reveals a three-stage mechanism of Na-intercalation to one of the state-of-the-art battery electrode materials operating in aqueous electrolytes.

A brief paragraph (no more than 200 words) that puts the work into the broader context

Na-ion batteries operating in aqueous media are among the most promising candidates to contribute to the solution of the so-called generation *vs* consumption problem in the future sustainable energy provision schemes, perhaps even at the "TW-level". However, in order to improve existing electrode materials in these devices, deeper fundamental understanding of processes governing their performance is necessary. In this work, it is shown that the interfacial transfer of sodium between one of the best cathode materials and aqueous electrolytes likely involves at least three stages. These stages are significantly influenced by the electrolyte properties and composition. The findings of this work can be used to design ever better Na-ion aqueous batteries, taking into account that the specific capacity of the optimised cathode systems in this work is just 5% lower if compared to the theoretical one at the C-rate as high as 180 C. Additionally, the role of solvation effects is emphasized.

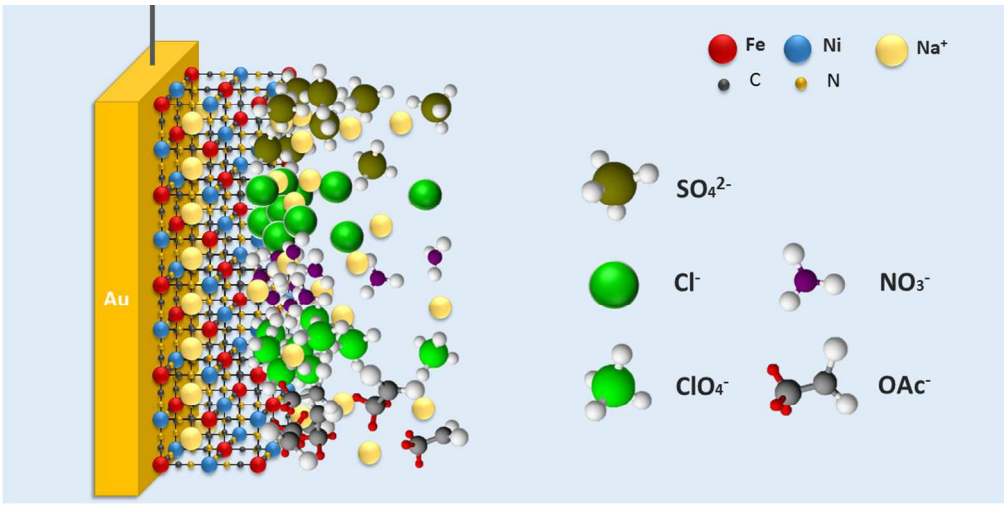

325x162mm (96 x 96 DPI)